

Knowing what you know in brain segmentation using deep neural networks

Patrick McClure^{a,c}, Nao Rho^{a,c}, John A. Lee^{b,c}, Jakub R. Kaczmarzyk^d, Charles Zheng^{a,c}, Satrajit S. Ghosh^d, Dylan Nielson^{b,c}, Adam Thomas^{b,c}, Peter Bandettini^c, Francisco Pereira^{a,c}

^a*Machine Learning Team, National Institute of Mental Health*

^b*Data Sharing and Science Team, National Institute of Mental Health*

^c*Section on Functional Imaging Methods, National Institute of Mental Health, Bg. 10 Rm. 1D80B 10 Center Dr., Bethesda, MD 20814*

^d*McGovern Institute for Brain Research, Massachusetts Institute of Technology, 46-4033F, 43 Vassar St, Cambridge, MA 02139*

Abstract

In this paper, we describe a deep neural network trained to predict FreeSurfer segmentations of structural MRI volumes, in seconds rather than hours. The network was trained and evaluated on the largest dataset ever assembled for this purpose, obtained by combining data from more than a hundred sites. We also show that the prediction uncertainty of the network at each voxel is a good indicator of whether the network has made an error. The resulting uncertainty volume can be used in conjunction with the predicted segmentation to improve downstream uses, such as calculation of measures derived from segmentation regions of interest or the building of prediction models. Finally, we demonstrate that the average prediction uncertainty across voxels in the brain is an excellent indicator of manual quality control ratings, outperforming the best available automated solutions.

1. Introduction

Segmentation of structural magnetic resonance imaging (sMRI) volumes is an essential processing step in many analyses of neuroimaging data. These segmentations are often generated using the FreeSurfer package [1], a process, which can take close to a day for each subject. The computational resources for doing

this at a scale of hundreds to thousands of subjects are beyond the capabilities of most sites. This has led to an interest in the use of deep neural networks as a general approach for learning to predict the outcome of a processing task, given the input data, in a much shorter time period than the processing would normally take. In particular, several deep neural networks have been trained to perform segmentation of brain sMRI volumes [2, 3, 4, 5, 6], taking between a few seconds and a few minutes per volume. These networks *directly* predict a manual or an automated segmentation from the structural volumes ([3, 4, 5] used FreeSurfer, [7] used GIF [8] instead to generate labels). These networks, however, have been trained on at most hundreds of examples from a limited number of sites, which can lead to poor cross-site generalization for complex segmentation tasks [9]. [3] used 581 sMRI volumes from the IXI dataset to train an initial model and then finetuned on 28 volumes from the MALC dataset [10]. They showed an approximately 9% average Dice loss on out-of-site data from the ADNI-29 [11], CANDI [12], and IBSR [13] datasets. [5] used 770 sMRI volumes from HCP [14] to train an initial model and then finetuned on 7 volumes from the FBIRN dataset [15]. [6] used 443 sMRI volumes from the ADNI dataset [7] for training. [5] and [7] did not report test results for sites that were not used during training.

These results show that it is possible to train a neural network to carry out segmentation of a structural image. However, they provide a limited indication of whether such a network would work on data from any new site not encountered in training. While finetuning on labelled data from new sites can improve performance, even while using small amounts of data [5, 3, 9], a robust neural network segmentation tool should generalize to new sites without any further effort. As part of the process of adding segmentation capabilities to the "no-brainer" tool ¹, we trained a network to predict FreeSurfer segmentations given a training set of more than 10,000 sMRI volumes. This paper describes this process, as well as a quantitative and qualitative evaluation of the performance

¹<https://github.com/kaczmarj/nobrainier>

of the resulting model.

Beyond the performance of the model, a second aspect of interest to us is to understand whether it is feasible for a network to indicate how confident it is about its prediction at each location in the brain. We expect the network to make errors, be it because of noise, unusual positioning of the brain, very different contrast than what it was trained on, etc. Because our model is probabilistic and seeks to learn uncertainties, we expect it to be less confident in its predictions in such cases. [6] showed that the accuracy of segmentation predictions was higher for voxels with low dropout sampling-based uncertainties. However, this type of uncertainty calculation significantly increases the time to produce a segmentation; furthermore, they only reported results for in-site test examples. In this paper, we evaluate the feasibility of using simpler uncertainty estimates for this purpose, both with in-site and out-of-site test data.

Finally, we test the hypothesis that overall prediction uncertainty across an entire image reflects its "quality", as measured by human quality control (QC) scores. Given the effort required to produce such scores, there have been multiple attempts to either crowdsource the process [16] or automate it [17]. The latter, in particular, does not rely on segmentation information, so we believe it is worthwhile to test whether uncertainty derived from segmentation is more effective.

2. Methods

2.1. Data

2.1.1. Imaging Datasets

We combined several datasets into a single dataset with 11,148 sMRI volumes. Most of these datasets contained data from multiple scanning sites. The joint dataset comprised 611 volumes from the CMI dataset [18], 3039 volumes from the CoRR dataset [19], 152 volumes from the GSP dataset [20], 956 volumes from the HCP dataset [14], 178 volumes from the HNBSSI dataset [21], 10 volumes from the Barrios dataset [22], 1,136 volumes from the NKI dataset [23],

477 volumes from the SALD [24], 1,003 volumes from the SLIM dataset, 992 volumes from the ABIDE dataset [25], 719 volumes from the ADHD200 dataset [26], 183 volumes from the Buckner Lab dataset [27], 45 volumes from the ICBM dataset [28], 51 volumes from the Gobbini Lab datasets [29], 55 volumes from the Haxby Lab datasets [30, 31], and 1,873 volumes from the OpenfMRI dataset [32]. The OpenfMRI data included volumes from [33, 34, 35, 36, 37, 38, 39, 40, 41, 42, 43, 44, 45, 46, 47, 48, 49, 50, 51, 52, 53, 54, 55, 56, 57, 58, 59, 60, 61, 62, 63, 64, 65, 66, 67, 68, 69, 70, 71, 72, 73, 74, 75, 76, 31, 77, 78, 79, 80, 81, 82, 83, 84, 85, 86]. An in-site test set was created from the combined dataset using a 90-10 training-test split.

We additionally used 440 sMRI volumes from the NNDSP dataset [87] as a held-out dataset to test generalization of the network to an unseen site. In addition to sMRI volumes, each NNDSP sMRI volume was given a QC score from 1 to 4, higher scores corresponding to worse scan quality, by two raters (3 if values differed by more than 1), as described in [88]. If a volume had a QC score greater than 2, it was labeled as a bad quality scan; otherwise, the scan was labeled as a good quality scan.

2.1.2. Data Preprocessing

All structural MRI datasets were collected with MPRAGE sequences, with a grid of $128 \times 128 \times 128$ mm^3 voxels. The only pre-processing that we performed was conforming the input sMRIs with FreeSurfer’s `mri_convert`, by resizing all of the volumes used to $256 \times 256 \times 256$ $1 mm^3$ voxels. During training and testing, input volumes were individually z-scored across voxels.

2.1.3. Segmentation Target

We computed 50-class FreeSurfer [1] segmentations, as in [5], for all subjects in each of the datasets described earlier. These were used as the labels for prediction. Although, FreeSurfer segmentations may not be perfectly correct, as compared to manual, expert segmentations, using them allowed us to create a large training dataset, as one could not feasibly label it by hand. FreeSurfer

trained networks can also outperform FreeSurfer segmentations when compared to expert segmentations [3]. The trained network could be finetuned with expert small amounts of labeled data, which would likely improve the results [3, 9].

2.2. Convolutional Neural Network

2.2.1. Architecture

Several deep neural network architectures have been proposed for brain segmentation, such as U-net [2], QuickNAT [3], HighResNet [6] and MeshNet [4, 5]. We chose MeshNet because of its relatively simple structure, its lower number of learned parameters, and its competitive performance.

MeshNet uses dilated convolutional layers [89] due to the 3D structural nature of sMRI data. The output of these discrete volumetric dilated convolutional layers can be expressed as:

$$(\mathbf{w}_f *_{l} \mathbf{h})_{i,j,k} = \sum_{\tilde{i}=-a}^a \sum_{\tilde{j}=-b}^b \sum_{\tilde{k}=-c}^c w_{f,\tilde{i},\tilde{j},\tilde{k}} h_{i-l\tilde{i},j-l\tilde{j},k-l\tilde{k}}. \quad (1)$$

where h is the input to the layer, a , b , and c are the bounds for the i , j , and k axes of the filter with weights \mathbf{w}_f , (i, j, k) is the voxel, \mathbf{v} , where the convolution is computed. The dilation factor l allows the convolution kernel to operate on every l -th voxel, since adjacent voxels are expected to be highly correlated. The dilation factor, number of filters, and other details of the MeshNet-like architecture that we used for all experiments is shown in Table 1.

We split each structural image into 512 non-overlapping $32 \times 32 \times 32$ sub-volumes, similarly to [4, 5], to be used as inputs for the neural network. The prediction target is the corresponding segmentation sub-volume. After generating segmentations for all 512 sub-volumes, these are then assembled into a segmentation of the entire structural image.

2.2.2. Maximum a Posteriori Estimation

When training a neural network, the weights of the network, \mathbf{w} are often learned using maximizing maximum likelihood estimation (MLE). For MLE,

Layer	Filter	Padding	Dilation (l)	Non-linearity
1	72×3^3	1	1	ReLU
2	72×3^3	1	1	ReLU
3	72×3^3	1	1	ReLU
4	72×3^3	2	2	ReLU
5	72×3^3	4	4	ReLU
6	72×3^3	8	8	ReLU
7	72×3^3	1	1	ReLU
8	50×1^3	0	1	Softmax

Table 1: The Meshnet dilated convolutional neural network architecture used for brain segmentation.

$\log p(\mathcal{D}|\mathbf{w})$ is maximized where $\mathcal{D} = \{(\mathbf{x}_1, \mathbf{y}_1), \dots, (\mathbf{x}_N, \mathbf{y}_N)\}$ is the training dataset and $(\mathbf{x}_n, \mathbf{y}_n)$ is the n th input-output example. This often overfits, however, so we used a prior on the network weights, $p(\mathbf{w})$, to obtain a maximum a posteriori (MAP) estimate, by optimizing $\log p(\mathbf{w}|\mathcal{D})$:

$$\operatorname{argmax}_{\mathbf{w}} \sum_{n=1}^N \log p(\mathbf{y}_n|\mathbf{x}_n, \mathbf{w}) - \log p(\mathbf{w}). \quad (2)$$

We used a fully factorized Gaussian prior (i.e. $p(w_{f,\bar{i},\bar{j},\bar{k}}) = \mathcal{N}(0, 1)$). This resulted in the weights being learned by minimizing the softmax cross-entropy with L2 regularization.

2.3. Quantifying performance

2.3.1. Segmentation performance measure

To measure the quality of the produced segmentations, we calculated the Dice coefficient, which is defined by

$$Dice_c = \frac{2|\hat{\mathbf{y}}_c \cdot \mathbf{y}_c|}{\|\hat{\mathbf{y}}_c\|^2 + \|\mathbf{y}_c\|^2} = \frac{2TP_c}{2TP_c + FN_c + FP_c}, \quad (3)$$

where $\hat{\mathbf{y}}_c$ is the binary segmentation for class c produced by a network, \mathbf{y}_c is the ground truth produced by FreeSurfer, TP_c is the true positive rate for class c ,

FN_c is the false negative rate for class c , and FP_c is the false positive rate for class c . We calculate the Dice coefficient separately for each class $c = 1, \dots, 50$, and average across classes to compute the overall performance of a network for one structural image.

2.3.2. Uncertainty measure

We quantify the uncertainty of a prediction, $p(\mathbf{y}_{m,c}|x_m, \mathbf{w})$ as the entropy of the softmax across the 50 output classes, $\sum_{c=1}^{50} p(\mathbf{y}_{m,c}|x_m, \mathbf{w}) \log p(\mathbf{y}_{m,c}|x_m, \mathbf{w})$. We calculate the uncertainty for each output voxel separately, and the uncertainty for one structural image by averaging across all output voxels not classified as background.

3. Results

3.1. Segmentation performance

We applied our network to produce segmentations for both the in-site test set and the out-of-site NNDSP data. Considering average Dice across all 50 classes for each structural image, the mean performance was ~ 0.78 and ~ 0.73 for the in-site and NNDSP data, respectively. This was significantly different by a paired t-test comparing the samples of mean Dice score for each of the 50 classes ($p = 7.28e - 14$). The distribution of Dice scores for each of the 50 classes, in both datasets, is shown in Figure 1. To evaluate the degree to which segmentation performance across the 50 classes was consistent between the two datasets, we computed the correlation between the mean Dice scores in each. The Pearson correlation was ~ 0.95 ($p = 2.99e - 26$ for $H_0 : \rho = 0$).

In Figures 2 and 3, we show selected example segmentations for the trained network for volumes that have Dice scores similar to the average Dice score across their respective dataset.

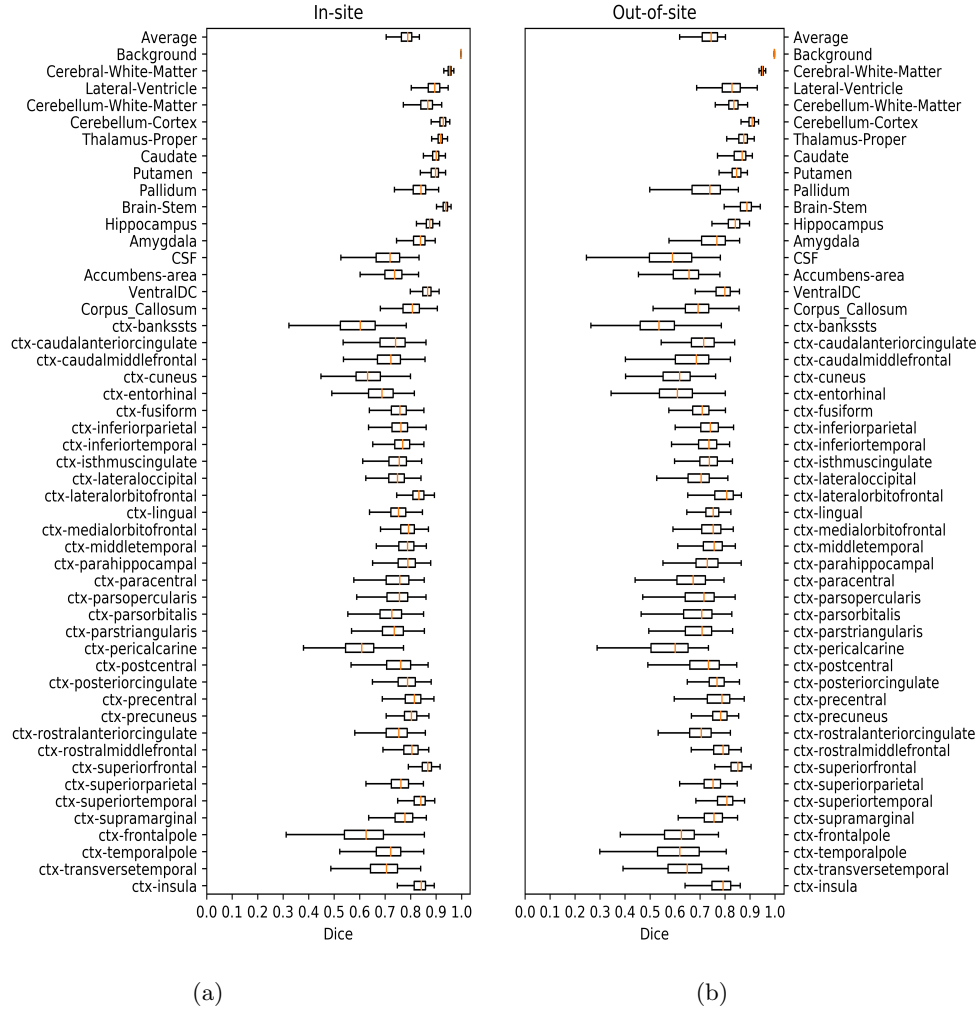


Figure 1: Boxplots of the the average Dice score and the scores for the 50 classes for (a) the in-site test set and (b) the NNDSF out-of-site test set.

3.2. Quantification of uncertainty

3.2.1. Predicting segmentation errors from uncertainty

Ideally, an increase in DNN prediction uncertainty indicates an increase in the likelihood that that prediction is incorrect. To evaluate whether this is the case for the trained brain segmentation DNN, we performed a receiver operating characteristic (ROC) analysis. In this analysis, voxels are ranked from most

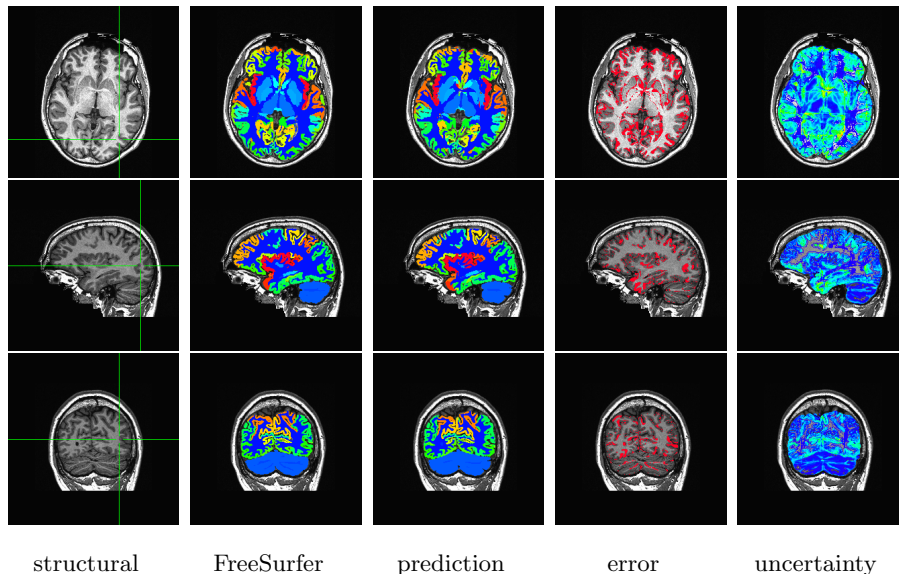


Figure 2: In-site segmentation results for a subject with average Dice performance. The columns show, respectively, the structural image used as input, the FreeSurfer segmentation used as a prediction target, the prediction made by our network, the voxels where there was a mismatch between prediction and target, and the prediction uncertainty at each voxel.

uncertain to least uncertain and one considers, at each rank, what fraction of the voxels were also misclassified by the network. This yields a curve, shown for both in-site test set and the held-out NNDSP dataset in Figure 4). Each curve is typically summarized by the area under it (AUC), resulting in AUCs of 0.8671 and 0.8555 for the in-site and NNDSP out-of-site data, respectively.

3.2.2. Predicting image quality from uncertainty

Ideally, the output uncertainty for inputs not drawn from the training distribution should be relatively high. This could potentially be useful for a variety of applications. One particular application is detection of bad quality sMRI scans, since the segmentation DNN was trained using relatively good quality scans. To test the validity of predicting high vs low quality scans, we performed an ROC analysis on the held-out NNDSP dataset, where manual quality control ratings are available. We also did the same analysis using MRIQC [17], the

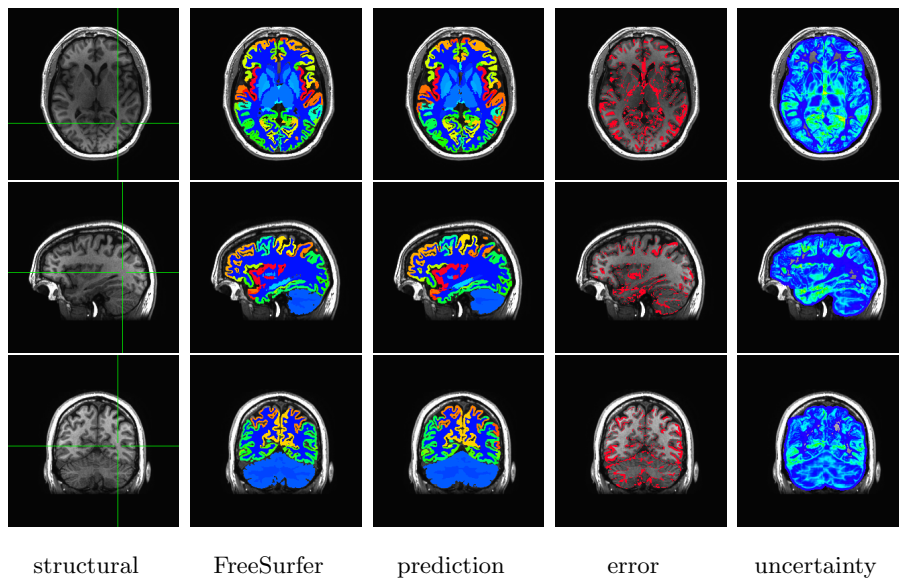


Figure 3: Out-of-site segmentation results for a subject with average Dice performance. The columns show, respectively, the structural image used as input, the FreeSurfer segmentation used as a prediction target, the prediction made by our network, the voxels where there was a mismatch between prediction and target, and the prediction uncertainty at each voxel.

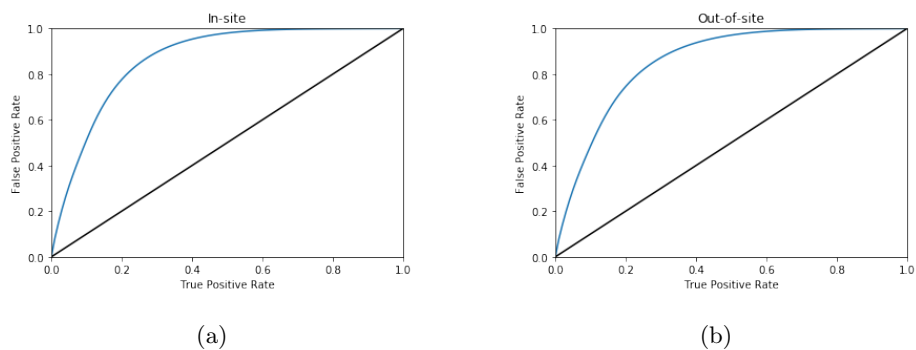


Figure 4: The average receiver operating characteristic (ROC) curves over test volumes for predicting the misclassification of a voxel from its uncertainty for (a) the in-site test set and (b) the NNDSP out-of-site test set.

best available automated method. The average uncertainty score derived from segmentation network uncertainty had an AUC of 0.8431, whereas the MRIQC scores had an AUC of 0.6061 (Figure 5).

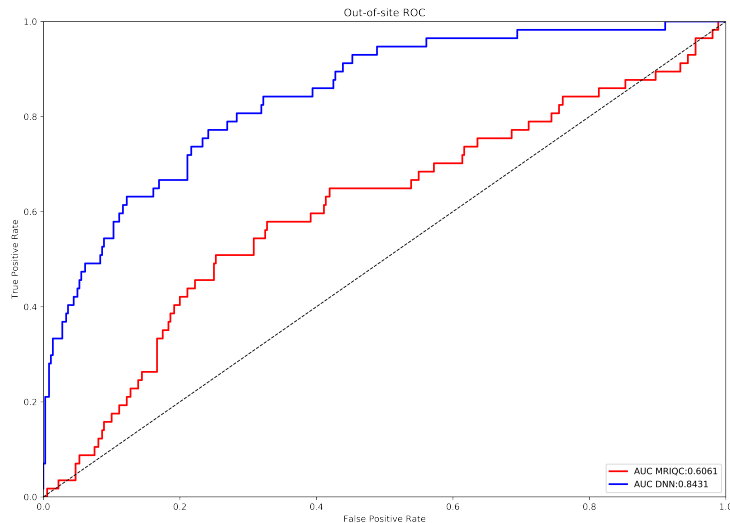


Figure 5: Receiver operating characteristic (ROC) curves for predicting scan quality from the average non-background voxel uncertainty and from MRIQC scores for the NNDSP out-of-site test set.

4. Discussion

We trained a deep neural network to predict FreeSurfer segmentations from structural MRI (sMRI) volumes. We trained on more than 10,000 sMRIs, obtained by combining 70 different datasets (many of which, in turn, contain images from several sites, e.g. NKI, ABIDE, ADHD200). We used a separate test set of more than 1,000 sMRIs, drawn from the same datasets. The resulting network performs at the same level of state-of-the-art networks [5]. This result, however, is obtained by testing over two orders of magnitude more test data, and many more sites, than those papers. This suggests that this may be the level of performance attainable with MeshNet or QuickNAT, absent some of the techniques we describe as possible future work below. We also test performance on a completely separate dataset from a site not encountered in training. Whereas Dice performance drops slightly (by 4.5%), this is less than what was observed in other studies (9% [3]); this suggests that we may be achieving better generalization by training on our dataset, and we plan on testing this on more

datasets from novel sites. This is particularly important to us, as this network is meant to be used in an off-the-shelf tool.

We believe it may be possible to improve this segmentation processing, in that we did not use *any* pre-processing, such as positioning the brain so that it was centered or had a vertical ACPC line. One option would be to use various techniques for data augmentation (e.g. variation of image contrast, since that is pretty heterogeneous, rotations/translations of existing examples, addition of realistic noise, etc). Another would be to eliminate the need to divide the brain into sub-volumes, which loses some global information; this will become more feasible in GPUs with more memory. Finally, we plan on using post-processing of results (e.g. ensure some coherence between predictions for adjacent voxels, leverage off-the-shelf brain and tissue masking code).

We demonstrated that the estimated uncertainty for the prediction at each voxel is a good indicator of whether the network makes an error in it, both in-site and out-of-site. The tool that produces the predicted segmentation volume for an input sMRI will also produce an uncertainty volume. We anticipate this being useful at various levels, e.g. to refine other tools that rely on segmentation images, or to improve prediction models based on sMRI data (e.g. modification of calculation of cortical thickness, surface area, voxel selection or weighting in regression or classification models, etc).

Finally, our results demonstrate that the average prediction uncertainty across voxels in the brain is an excellent indicator of manual quality control ratings. Furthermore, it outperforms the best existing automated solution [17]. Since automation is already used in large repositories (e.g. OpenMRI), we plan on offering our tool as an additional quality control measure.

References

References

- [1] B. Fischl, Freesurfer, Neuroimage 62 (2).

- [2] O. Ronneberger, P. Fischer, T. Brox, U-net: Convolutional networks for biomedical image segmentation, in: International Conference on Medical Image Computing and Computer-Assisted Intervention, Springer, 2015, pp. 234–241.
- [3] A. G. Roy, S. Conjeti, N. Navab, C. Wachinger, QuickNAT: Segmenting MRI neuroanatomy in 20 seconds, arXiv preprint arXiv:1801.04161.
- [4] A. Fedorov, J. Johnson, E. Damaraju, A. Ozerin, V. Calhoun, S. Plis, End-to-end learning of brain tissue segmentation from imperfect labeling, in: International Joint Conference on Neural Networks, IEEE, 2017, pp. 3785–3792.
- [5] A. Fedorov, E. Damaraju, V. Calhoun, S. Plis, Almost instant brain atlas segmentation for large-scale studies, arXiv preprint arXiv:1711.00457.
- [6] W. Li, G. Wang, L. Fidon, S. Ourselin, M. J. Cardoso, T. Vercauteren, On the compactness, efficiency, and representation of 3D convolutional networks: Brain parcellation as a pretext task, in: International Conference on Information Processing in Medical Imaging, Springer, 2017, pp. 348–360.
- [7] R. C. Petersen, P. Aisen, L. Beckett, M. Donohue, A. Gamst, D. Harvey, C. Jack, W. Jagust, L. Shaw, A. Toga, et al., Alzheimer’s disease neuroimaging initiative (adni): clinical characterization, *Neurology* 74 (3) (2010) 201–209.
- [8] M. J. Cardoso, M. Modat, R. Wolz, A. Melbourne, D. Cash, D. Rueckert, S. Ourselin, Geodesic information flows: spatially-variant graphs and their application to segmentation and fusion, *IEEE transactions on medical imaging* 34 (9) (2015) 1976–1988.
- [9] P. McClure, C. Y. Zheng, J. Kaczmarzyk, J. Rogers-Lee, S. Ghosh, D. Nielson, P. A. Bandettini, F. Pereira, Distributed weight consolidation: A brain segmentation case study, in: S. Bengio, H. Wallach, H. Larochelle, K. Grau-

- man, N. Cesa-Bianchi, R. Garnett (Eds.), *Advances in Neural Information Processing Systems* 31, 2018, pp. 4093–4103.
- [10] D. S. Marcus, T. H. Wang, J. Parker, J. G. Csernansky, J. C. Morris, R. L. Buckner, Open access series of imaging studies (oasis): cross-sectional mri data in young, middle aged, nondemented, and demented older adults, *Journal of cognitive neuroscience* 19 (9) (2007) 1498–1507.
- [11] S. G. Mueller, M. W. Weiner, L. J. Thal, R. C. Petersen, C. Jack, W. Jagust, J. Q. Trojanowski, A. W. Toga, L. Beckett, The alzheimer’s disease neuroimaging initiative, *Neuroimaging Clinics* 15 (4) (2005) 869–877.
- [12] D. N. Kennedy, C. Haselgrove, S. M. Hodge, P. S. Rane, N. Makris, J. A. Frazier, Candishare: a resource for pediatric neuroimaging data (2012).
- [13] T. Rohlfing, Image similarity and tissue overlaps as surrogates for image registration accuracy: widely used but unreliable, *IEEE transactions on medical imaging* 31 (2) (2012) 153–163.
- [14] D. C. Van Essen, S. M. Smith, D. M. Barch, T. E. Behrens, E. Yacoub, K. Ugurbil, W.-M. H. Consortium, et al., The WU-Minn human connectome project: An overview, *NeuroImage* 80 (2013) 62–79.
- [15] D. B. Keator, T. G. van Erp, J. A. Turner, G. H. Glover, B. A. Mueller, T. T. Liu, J. T. Voyvodic, J. Rasmussen, V. D. Calhoun, H. J. Lee, et al., The function biomedical informatics research network data repository, *Neuroimage* 124 (2016) 1074–1079.
- [16] A. Keshavan, J. Yeatman, A. Rokem, Combining citizen science and deep learning to amplify expertise in neuroimaging, *bioRxiv*:<https://www.biorxiv.org/content/early/2018/07/06/363382.full.pdf>, doi: 10.1101/363382.
URL <https://www.biorxiv.org/content/early/2018/07/06/363382>

- [17] O. Esteban, D. Birman, M. Schaer, O. O. Koyejo, R. A. Poldrack, K. J. Gorgolewski, Mriqc: Advancing the automatic prediction of image quality in mri from unseen sites, *PloS one* 12 (9) (2017) e0184661.
- [18] L. M. Alexander, J. Escalera, L. Ai, C. Andreotti, K. Febré, A. Mangone, N. Vega-Potler, N. Langer, A. Alexander, M. Kovacs, et al., An open resource for transdiagnostic research in pediatric mental health and learning disorders, *Scientific data* 4 (2017) 170181.
- [19] X.-N. Zuo, J. S. Anderson, P. Bellec, R. M. Birn, B. B. Biswal, J. Blautzik, J. C. Breitner, R. L. Buckner, V. D. Calhoun, F. X. Castellanos, et al., An open science resource for establishing reliability and reproducibility in functional connectomics, *Scientific data* 1 (2014) 140049.
- [20] A. J. Holmes, M. O. Hollinshead, T. M. OKeefe, V. I. Petrov, G. R. Fariello, L. L. Wald, B. Fischl, B. R. Rosen, R. W. Mair, J. L. Roffman, et al., Brain genomics superstruct project initial data release with structural, functional, and behavioral measures, *Scientific data* 2 (2015) 150031.
- [21] D. OConnor, N. V. Potler, M. Kovacs, T. Xu, L. Ai, J. Pellman, T. Vanderwal, L. C. Parra, S. Cohen, S. Ghosh, et al., The healthy brain network serial scanning initiative: a resource for evaluating inter-individual differences and their reliabilities across scan conditions and sessions, *Gigascience* 6 (2) (2017) 1–14.
- [22] P. G. Viquez, S. Whitfield-Gabrieli, C. C. Bauer, Barrios, F. A., Brain functional connectivity of hypnosis without target suggestion. an intrinsic hypnosis rs-fmri study., (under review).
- [23] K. B. Nooner, S. Colcombe, R. Tobe, M. Mennes, M. Benedict, A. Moreno, L. Panek, S. Brown, S. Zavitz, Q. Li, et al., The NKI-Rockland sample: A model for accelerating the pace of discovery science in psychiatry, *Frontiers in Neuroscience* 6 (2012) 152.

- [24] D. Wei, K. Zhuang, Q. Chen, W. Yang, W. Liu, K. Wang, J. Sun, J. Qiu, Structural and functional mri from a cross-sectional southwest university adult lifespan dataset (sald), *bioRxiv* (2018) 177279.
- [25] A. Di Martino, C.-G. Yan, Q. Li, E. Denio, F. X. Castellanos, K. Alaerts, J. S. Anderson, M. Assaf, S. Y. Bookheimer, M. Dapretto, et al., The autism brain imaging data exchange: Towards a large-scale evaluation of the intrinsic brain architecture in autism, *Molecular Psychiatry* 19 (6) (2014) 659.
- [26] P. Bellec, C. Chu, F. Chouinard-Decorte, Y. Benhajali, D. S. Margulies, R. C. Craddock, The neuro bureau adhd-200 preprocessed repository, *Neuroimage* 144 (2017) 275–286.
- [27] B. B. Biswal, M. Mennes, X.-N. Zuo, S. Gohel, C. Kelly, S. M. Smith, C. F. Beckmann, J. S. Adelstein, R. L. Buckner, S. Colcombe, et al., Toward discovery science of human brain function, *Proceedings of the National Academy of Sciences* 107 (10) (2010) 4734–4739.
- [28] J. Mazziotta, A. Toga, A. Evans, P. Fox, J. Lancaster, K. Zilles, R. Woods, T. Paus, G. Simpson, B. Pike, et al., A probabilistic atlas and reference system for the human brain: International consortium for brain mapping (icbm), *Philosophical Transactions of the Royal Society of London B: Biological Sciences* 356 (1412) (2001) 1293–1322.
- [29] M. V. di Oleggio Castello, Y. O. Halchenko, J. S. Guntupalli, J. D. Gors, M. I. Gobbini, The neural representation of personally familiar and unfamiliar faces in the distributed system for face perception, *Scientific Reports* 7.
- [30] J. V. Haxby, J. S. Guntupalli, A. C. Connolly, Y. O. Halchenko, B. R. Conroy, M. I. Gobbini, M. Hanke, P. J. Ramadge, A common, high-dimensional model of the representational space in human ventral temporal cortex, *Neuron* 72 (2) (2011) 404–416.

- [31] S. A. Nastase, A. C. Connolly, N. N. Oosterhof, Y. O. Halchenko, J. S. Guntupalli, M. Visconti di Oleggio Castello, J. Gors, M. I. Gobbini, J. V. Haxby, Attention selectively reshapes the geometry of distributed semantic representation, *Cerebral Cortex* 27 (8) (2017) 4277–4291.
- [32] R. A. Poldrack, D. M. Barch, J. Mitchell, T. Wager, A. D. Wagner, J. T. Devlin, C. Cumba, O. Koyejo, M. Milham, Toward open sharing of task-based fmri data: the openfmri project, *Frontiers in neuroinformatics* 7 (2013) 12.
- [33] T. Schonberg, C. R. Fox, J. A. Mumford, E. Congdon, C. Trepel, R. A. Poldrack, Decreasing ventromedial prefrontal cortex activity during sequential risk-taking: an fmri investigation of the balloon analog risk task, *Frontiers in neuroscience* 6 (2012) 80.
- [34] A. R. Aron, M. A. Gluck, R. A. Poldrack, Long-term test–retest reliability of functional mri in a classification learning task, *Neuroimage* 29 (3) (2006) 1000–1006.
- [35] S. M. Tom, C. R. Fox, C. Trepel, R. A. Poldrack, The neural basis of loss aversion in decision-making under risk, *Science* 315 (5811) (2007) 515–518.
- [36] G. Xue, A. R. Aron, R. A. Poldrack, Common neural substrates for inhibition of spoken and manual responses, *Cerebral Cortex* 18 (8) (2008) 1923–1932.
- [37] A. R. Aron, T. E. Behrens, S. Smith, M. J. Frank, R. A. Poldrack, Triangulating a cognitive control network using diffusion-weighted magnetic resonance imaging (mri) and functional mri, *Journal of Neuroscience* 27 (14) (2007) 3743–3752.
- [38] K. Foerde, B. J. Knowlton, R. A. Poldrack, Modulation of competing memory systems by distraction, *Proceedings of the National Academy of Sciences* 103 (31) (2006) 11778–11783.

- [39] A. C. Kelly, L. Q. Uddin, B. B. Biswal, F. X. Castellanos, M. P. Milham, Competition between functional brain networks mediates behavioral variability, *Neuroimage* 39 (1) (2008) 527–537.
- [40] M. Mennes, C. Kelly, X.-N. Zuo, A. Di Martino, B. B. Biswal, F. X. Castellanos, M. P. Milham, Inter-individual differences in resting-state functional connectivity predict task-induced bold activity, *Neuroimage* 50 (4) (2010) 1690–1701.
- [41] M. Mennes, X.-N. Zuo, C. Kelly, A. Di Martino, Y.-F. Zang, B. Biswal, F. X. Castellanos, M. P. Milham, Linking inter-individual differences in neural activation and behavior to intrinsic brain dynamics, *Neuroimage* 54 (4) (2011) 2950–2959.
- [42] S. J. Hanson, T. Matsuka, J. V. Haxby, Combinatorial codes in ventral temporal lobe for object recognition: Haxby (2001) revisited: is there a face area?, *Neuroimage* 23 (1) (2004) 156–166.
- [43] A. J. O’toole, F. Jiang, H. Abdi, J. V. Haxby, Partially distributed representations of objects and faces in ventral temporal cortex, *Journal of cognitive neuroscience* 17 (4) (2005) 580–590.
- [44] K. J. Duncan, C. Pattamadilok, I. Knierim, J. T. Devlin, Consistency and variability in functional localisers, *Neuroimage* 46 (4) (2009) 1018–1026.
- [45] T. D. Wager, M. L. Davidson, B. L. Hughes, M. A. Lindquist, K. N. Ochsner, Prefrontal-subcortical pathways mediating successful emotion regulation, *Neuron* 59 (6) (2008) 1037–1050.
- [46] J. M. Moran, E. Jolly, J. P. Mitchell, Social-cognitive deficits in normal aging, *Journal of neuroscience* 32 (16) (2012) 5553–5561.
- [47] M. R. Uncapher, J. B. Hutchinson, A. D. Wagner, Dissociable effects of top-down and bottom-up attention during episodic encoding, *Journal of Neuroscience* 31 (35) (2011) 12613–12628.

- [48] K. J. Gorgolewski, A. Storkey, M. E. Bastin, I. R. Whittle, J. M. Wardlaw, C. R. Pernet, A test-retest fmri dataset for motor, language and spatial attention functions, *GigaScience* 2 (1) (2013) 6.
- [49] G. Repovs, D. M. Barch, Working memory related brain network connectivity in individuals with schizophrenia and their siblings, *Frontiers in human neuroscience* 6 (2012) 137.
- [50] J. M. Walz, R. I. Goldman, M. Carapezza, J. Muraskin, T. R. Brown, P. Sajda, Simultaneous eeg-fmri reveals temporal evolution of coupling between supramodal cortical attention networks and the brainstem, *Journal of Neuroscience* 33 (49) (2013) 19212–19222.
- [51] K. Velanova, M. E. Wheeler, B. Luna, Maturation changes in anterior cingulate and frontoparietal recruitment support the development of error processing and inhibitory control, *Cerebral Cortex* 18 (11) (2008) 2505–2522.
- [52] A. Padmanabhan, C. F. Geier, S. J. Ordaz, T. Teslovich, B. Luna, Developmental changes in brain function underlying the influence of reward processing on inhibitory control, *Developmental cognitive neuroscience* 1 (4) (2011) 517–529.
- [53] N. Cera, A. Tartaro, S. L. Sensi, Modafinil alters intrinsic functional connectivity of the right posterior insula: a pharmacological resting state fmri study, *PLoS One* 9 (9) (2014) e107145.
- [54] T. D. Verstynen, The organization and dynamics of corticostriatal pathways link the medial orbitofrontal cortex to future behavioral responses, *Journal of neurophysiology* 112 (10) (2014) 2457–2469.
- [55] E. Gabitov, D. Manor, A. Karni, Patterns of modulation in the activity and connectivity of motor cortex during the repeated generation of movement sequences, *Journal of cognitive neuroscience* 27 (4) (2015) 736–751.

- [56] E. Gabitov, D. Manor, A. Karni, Done that: short-term repetition related modulations of motor cortex activity as a stable signature for overnight motor memory consolidation, *Journal of cognitive neuroscience* 26 (12) (2014) 2716–2734.
- [57] R. J. Lepping, R. A. Atchley, E. Chrysikou, L. E. Martin, A. A. Clair, R. E. Ingram, W. K. Simmons, C. R. Savage, Neural processing of emotional musical and nonmusical stimuli in depression, *PloS one* 11 (6) (2016) e0156859.
- [58] A.-L. Hsu, K.-H. Chou, Y.-P. Chao, H.-Y. Fan, C. W. Wu, J.-H. Chen, Physiological contribution in spontaneous oscillations: an approximate quality-assurance index for resting-state fmri signals, *PloS one* 11 (2) (2016) e0148393.
- [59] L. Koenders, J. Cousijn, W. A. Vingerhoets, W. van den Brink, R. W. Wiers, C. J. Meijer, M. W. Machielsen, D. J. Veltman, A. E. Goudriaan, L. de Haan, Grey matter changes associated with heavy cannabis use: a longitudinal smri study, *PLoS One* 11 (5) (2016) e0152482.
- [60] E. Iannilli, R. Gasparotti, T. Hummel, S. Zoni, C. Benedetti, C. Fedrighi, C. Y. Tang, C. Van Thriel, R. G. Lucchini, Effects of manganese exposure on olfactory functions in teenagers: a pilot study, *PloS one* 11 (1) (2016) e0144783.
- [61] G. Nilsson, S. Tamm, P. d’Onofrio, H. Å. Thuné, J. Schwarz, C. Lavebratt, J. J. Liu, K. N. Månsson, T. Sundelin, J. Axelsson, et al., A multimodal brain imaging dataset on sleep deprivation in young and old humans.
- [62] P. Van Schuerbeek, C. Baeken, J. De Mey, The heterogeneity in retrieved relations between the personality trait harm avoidance and gray matter volumes due to variations in the vbm and roi labeling processing settings, *PloS one* 11 (4) (2016) e0153865.

- [63] C. Stephan-Otto, S. Siddi, C. Senior, D. Muñoz-Samons, S. Ochoa, A. M. Sánchez-Laforga, G. Brébion, Visual imagery and false memory for pictures: a functional magnetic resonance imaging study in healthy participants, *PloS one* 12 (1) (2017) e0169551.
- [64] D. Dickstein, M. Pullman, C. Fernandez, J. Short, L. Kostakoglu, K. Kne-saurek, L. Soleimani, B. Jordan, W. Gordon, K. Dams-O'Connor, et al., Cerebral [18 f] t807/av1451 retention pattern in clinically probable cte resembles pathognomonic distribution of cte tauopathy, *Translational psychiatry* 6 (9) (2016) e900.
- [65] J. Kim, J. Wang, D. H. Wedell, S. V. Shinkareva, Identifying core affect in individuals from fmri responses to dynamic naturalistic audiovisual stimuli, *PloS one* 11 (9) (2016) e0161589.
- [66] V. a. Magnotta, J. T. Matsui, D. Liu, H. J. Johnson, J. D. Long, B. D. Bolster, B. a. Mueller, K. O. Lim, S. Mori, K. Helmer, J. a. Turner, M. J. Lowe, E. Aylward, L. a. Flashman, G. Bonett, J. S. Paulsen, Multi-Center Reliability of Diffusion Tensor Imaging, *Brain Connectivity* 2 (6) (2012) 121018043201009.
- [67] E. DuPre, W.-M. Luh, R. N. Spreng, Multi-echo fmri replication sample of autobiographical memory, prospection and theory of mind reasoning tasks, *Scientific data* 3 (2016) 160116.
- [68] X. Gao, X. Deng, X. Wen, Y. She, P. C. Vinke, H. Chen, My body looks like that girls: Body mass index modulates brain activity during body image self-reflection among young women, *PloS one* 11 (10) (2016) e0164450.
- [69] L. Romaniuk, M. Pope, K. Nicol, D. Steele, J. Hall, Neural correlates of fears of abandonment and rejection in borderline personality disorder, *Wellcome Open Research* 1.
- [70] A. J. Chanales, A. Oza, S. E. Favila, B. A. Kuhl, Overlap among spa-

tial memories triggers repulsion of hippocampal representations, *Current Biology* 27 (15) (2017) 2307–2317.

- [71] J. R. Dalenberg, L. Weitkamp, R. J. Renken, L. Nanetti, G. J. ter Horst, Flavor pleasantness processing in the ventral emotion network, *PloS one* 12 (2) (2017) e0170310.
- [72] A. Roy, R. A. Bernier, J. Wang, M. Benson, J. J. French Jr, D. C. Good, F. G. Hillary, The evolution of cost-efficiency in neural networks during recovery from traumatic brain injury, *PLoS One* 12 (4) (2017) e0170541.
- [73] T. H. FitzGerald, D. Hämmerer, K. J. Friston, S.-C. Li, R. J. Dolan, Sequential inference as a mode of cognition and its correlates in fronto-parietal and hippocampal brain regions, *PLoS computational biology* 13 (5) (2017) e1005418.
- [74] I. C. Ballard, B. Kim, A. Liatsis, G. Aydogan, J. D. Cohen, S. M. McClure, More is meaningful: the magnitude effect in intertemporal choice depends on self-control, *Psychological science* 28 (10) (2017) 1443–1454.
- [75] E. M. Gordon, T. O. Laumann, A. W. Gilmore, D. J. Newbold, D. J. Greene, J. J. Berg, M. Ortega, C. Hoyt-Drazen, C. Gratton, H. Sun, et al., Precision functional mapping of individual human brains, *Neuron* 95 (4) (2017) 791–807.
- [76] I. E. de Araujo, T. Lin, M. G. Veldhuizen, D. M. Small, Metabolic regulation of brain response to food cues, *Current Biology* 23 (10) (2013) 878–883.
- [77] S. A. Nastase, Y. O. Halchenko, A. C. Connolly, M. I. Gobbini, J. V. Haxby, Neural responses to naturalistic clips of behaving animals in two different task contexts, *Frontiers in neuroscience* 12 (2018) 316.
- [78] M. Vidorreta, Z. Wang, Y. V. Chang, D. A. Wolk, M. A. Fernández-Seara, J. A. Detre, Whole-brain background-suppressed pCASL MRI with

- 1d-accelerated 3d rare stack-of-spirals readout, *PloS one* 12 (8) (2017) e0183762.
- [79] A. Bischoff-Grethe, I. B. Ozyurt, E. Busa, B. T. Quinn, C. Fennema-Notestine, C. P. Clark, S. Morris, M. W. Bondi, T. L. Jernigan, A. M. Dale, et al., A technique for the deidentification of structural brain mr images, *Human brain mapping* 28 (9) (2007) 892–903.
- [80] J. Maclaren, Z. Han, S. B. Vos, N. Fischbein, R. Bammer, Reliability of brain volume measurements: A test-retest dataset, *Scientific data* 1 (2014) 140037.
- [81] M. Vidorreta, Z. Wang, I. Rodríguez, M. A. Pastor, J. A. Detre, M. A. Fernández-Seara, Comparison of 2d and 3d single-shot asl perfusion fmri sequences, *Neuroimage* 66 (2013) 662–671.
- [82] A. C. Connolly, J. S. Guntupalli, J. Gors, M. Hanke, Y. O. Halchenko, Y.-C. Wu, H. Abdi, J. V. Haxby, The representation of biological classes in the human brain, *Journal of Neuroscience* 32 (8) (2012) 2608–2618.
- [83] J. D. Power, M. Plitt, P. Kundu, P. A. Bandettini, A. Martin, Temporal interpolation alters motion in fmri scans: Magnitudes and consequences for artifact detection, *PloS one* 12 (9) (2017) e0182939.
- [84] F. Tadel, S. Baillet, J. C. Mosher, D. Pantazis, R. M. Leahy, Brainstorm: a user-friendly application for meg/eeg analysis, *Computational intelligence and neuroscience* 2011 (2011) 8.
- [85] A. Gramfort, M. Luessi, E. Larson, D. A. Engemann, D. Strohmeier, C. Brodbeck, L. Parkkonen, M. S. Hämäläinen, Mne software for processing meg and eeg data, *Neuroimage* 86 (2014) 446–460.
- [86] A. Gramfort, M. Luessi, E. Larson, D. A. Engemann, D. Strohmeier, C. Brodbeck, R. Goj, M. Jas, T. Brooks, L. Parkkonen, et al., Meg and eeg data analysis with mne-python, *Frontiers in neuroscience* 7 (2013) 267.

- [87] J. A. Lee, S. Gustavo, N. Migenishvili, D. Nielson, P. A. Bandettini, P. Shaw, A. Thomas, Automated quality control methods applied to a novel dataset., organization for Human Brain Mapping (OHBM) Annual Meeting (2018).
- [88] J. D. Blumenthal, A. Zijdenbos, E. Molloy, J. N. Giedd, Motion artifact in magnetic resonance imaging: implications for automated analysis, *Neuroimage* 16 (1) (2002) 89–92.
- [89] F. Yu, V. Koltun, Multi-scale context aggregation by dilated convolutions, in: International Conference on Learning Representations, 2015.